

# Beam-energy and system-size dependence of the CME

V.D Toneev<sup>1,2</sup> and V. Voronyuk<sup>1,3,4</sup>

<sup>1</sup> *Joint Institute for Nuclear Research, 141980 Dubna, Russia*

<sup>2</sup> *GSI, Helmholtzzentrum für Schwerionenforschung GmbH, 64291 Darmstadt, Germany*

<sup>3</sup> *Bogolyubov Institute for Theoretical Physics, 03680 Kiev, Ukraine*

<sup>4</sup> *Institute für Theoretische Physik, Universität Frankfurt, 60438 Germany*

## Abstract

The energy dependence of the local  $\mathcal{P}$  and  $\mathcal{CP}$  violation in Au+Au and Cu+Cu collisions in a large energy range is estimated within a simple phenomenological model. It is expected that at LHC the Chiral Magnetic effect (CME) will be about 20 times weaker than at RHIC. In the lower energy range this effect should vanish sharply at energy somewhere above the top SPS one. To elucidate CME background effects a transport model including magnetic field evolution is put forward.

## 1 Introduction

As was argued in Refs. [1, 2, 3, 4] the topological effects in QCD with induced chiral asymmetry may be observed in heavy ion collisions directly in the presence of very intense external electromagnetic fields due to the “Chiral Magnetic Effect” (CME) as a manifestation of spontaneous violation of the  $\mathcal{CP}$  symmetry. First experimental evidence for the CME identified via the observed charge separation effect with respect to the reaction plane has been presented by the STAR Collaboration [6]. In this paper we analyze the STAR data in a simple phenomenological way to estimate a possibility observing the CME in the larger energy range, from the LHC to FAIR/NICA energies. We also make a step towards a dynamical estimate of the CME background based on the nonequilibrium Hadron-String-Dynamics (HSD) microscopical transport approach [7] including magnetic field.

## 2 Phenomenological estimates of the CME

A characteristic scale of the process is given by the saturation momentum  $Q_s$  [1], so the transverse momentum of particles  $p_t \sim Q_s$ . Then the total

transverse energy per unit rapidity at mid-rapidity deposited at the formation of hot matter is expressed through the overlapping surface of two colliding nuclei in the transverse plane  $S$

$$\frac{dE_T}{dy} \sim \epsilon \cdot V = \epsilon \cdot \Delta z \cdot S = Q_s \cdot (Q_s^2 S) \sim Q_s \cdot \frac{dN_{\text{hadrons}}}{dy}. \quad (1)$$

Here the energy density and longitudinal size  $\Delta z \simeq \Delta\tau \simeq 1/Q_s$  are taken in order of magnitude as follows  $\epsilon \sim Q_s^4$  and  $\Delta z \sim 1/Q_s$ .

For one-dimensional random walk in the topological number space the topological charge (winding number) generated during the time  $\tau_B$ , when the magnetic field is present, may be estimated as

$$n_w \equiv \sqrt{Q_s^2} = \sqrt{\Gamma_S \cdot V \cdot \tau_B} \sim \sqrt{\frac{dN_{\text{hadrons}}}{dy}} \cdot \sqrt{Q_s \tau_B}, \quad (2)$$

where  $\Gamma_S$  is the sphaleron transition rate which in weak and strong coupling  $\Gamma_S \sim T^4$  with different coefficients. The initial temperature  $T_0$  of the produced matter at time  $\tau \simeq 1/Q_s$  is proportional to the saturation momentum  $Q_s$ ,  $T_0 = c Q_s$ . At the last step of (2) the expansion time and the corresponding time dependence of the temperature are neglected. Since sizable sphaleron transitions occur only in the deconfined phase, the time  $\tau_B$  in Eq. (2) is really the smallest lifetime between the strong magnetic field  $\tilde{\tau}_B$  one and the lifetime of deconfined matter  $\tau_\epsilon$ :

$$\tau_B = \min\{\tilde{\tau}_B, \tau_\epsilon\}. \quad (3)$$

The measured electric charge particle asymmetry is associated with the averaged correlator  $a$  by the following relation [8]:

$$\langle \cos(\psi_\alpha + \psi_\beta - 2\Psi_{RP}) \rangle = \langle \cos(\psi_\alpha + \psi_\beta - 2\psi_c) \rangle / v_{2,c} = v_{1,\alpha} v_{1,\beta} - a_\alpha a_\beta, \quad (4)$$

where  $\Psi_{RP}$  is the azimuthal angle of the reaction plane defined by the beam axis and the line joining the centers of colliding nuclei. Averaging in (4) is carried out over the whole event ensemble. The second equality in (4) corresponds to azimuthal measurements with respect to particle of type  $c$  extracted from three-body correlation analysis [8],  $v_1$  and  $v_2$  are the directed and elliptic flow parameters, respectively. According to Ref. [1] an average correlator  $a = \sqrt{a_\alpha a_\beta}$  is related to the topological charge,  $n_w$ , as

$$a \sim \frac{n_w}{dN_{\text{hadrons}}/dy} \sim \frac{\sqrt{Q_s \tau_B}}{\sqrt{dN_{\text{hadrons}}/dy}} \sim \sqrt{\frac{\tau_B}{Q_s}} \sim (\sqrt{s_{NN}})^{-1/16} \cdot \sqrt{\tau_B}, \quad (5)$$

where absorption and rescattering in dense matter responsible are neglected for the difference of magnitudes between the same and opposite charge correlations. In the last equality we assumed that  $Q_s^2 \sim s_{NN}^{1/8} \sim dN_{\text{hadrons}}/dy$  [9]. Our subsequent consideration is based on Eq. (5).

Thus, the direct energy dependence of average correlator is comparatively weak. Results of dynamical heavy-ion calculations of the magnetic field at the central point of the transverse overlapping region of colliding nuclei and energy density of created particles are presented in Figs. 1 and 2, respectively. Here for a field estimate we follow Ref. [10] basing on the UrQMD model [11] and applying the electromagnetic Lienard-Wiechert potential with the retardation condition for the magnetic field. As is seen, at the impact parameter  $b = 10$  fm the maximal strength of the dominant magnetic field component  $B_y$  (being perpendicular to the reaction plane) is decreased in Au+Au collisions by the factor of about 10, when one proceeds from  $\sqrt{s_{NN}} = 200$  GeV to  $E_{\text{lab}} = 11$  GeV, while for the created particle energy density  $\varepsilon$  in the central box this factor is 250, *i.e.* noticeably higher.

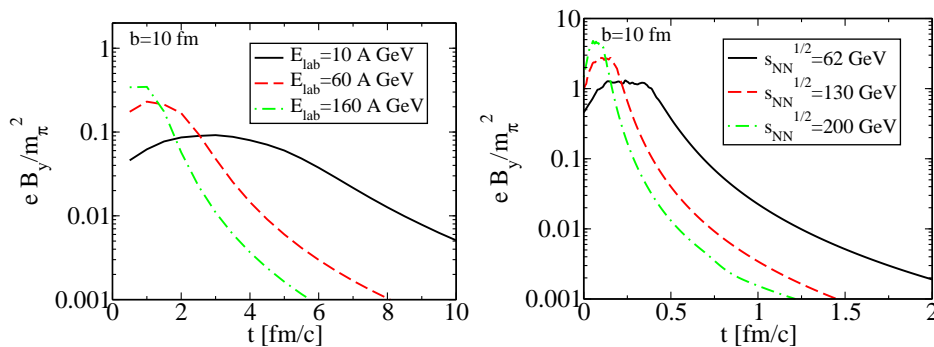


Figure 1: The time evolution of the magnetic field strength  $eB_y$  at the central region in Au+Au collisions with the impact parameter  $b = 10$  fm for different bombarding energies. Calculations are carried out within the UrQMD model [11] (for a detail see [10]).

To use Eq. (5) we need to identify the impact parameter, saturation momentum and multiplicity at a specific centrality. These can be found in Ref. [9] where the Glauber calculations were done. As a reference point we choose  $b = 10$  fm in our subsequent consideration.

The measured value of  $\langle \cos(\psi_\alpha + \psi_\beta - 2\Psi_{RP}) \rangle$  for the same charge particles from Au+Au ( $\sqrt{s_{NN}} = 200$  GeV) collisions at the impact parameter  $b = 10$  fm (40-50% centrality interval) is  $-(0.312 \pm 0.027) \cdot 10^{-3}$  [6]. Appropriate number for  $\sqrt{s_{NN}} = 62$  GeV seems to be a little bit larger but for Cu+Cu

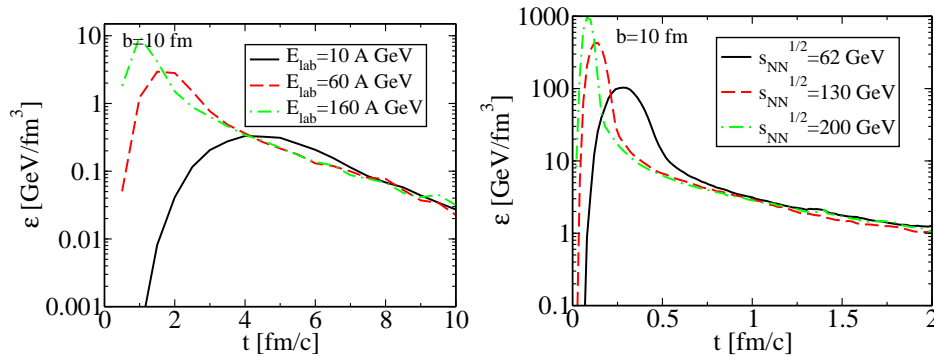


Figure 2: The time evolution of the energy density  $\varepsilon$  of created particles in the Lorentz-contracted box with the 2 fm side at the central point of overlapping region. The impact parameter  $b = 10$  fm.

collisions the effect is definitely stronger [6]. Thus, ignoring any final state interactions with medium, assuming  $a_\alpha = a_\beta = a$  and neglecting the directed flow  $v_{1a} = v_{1b} = 0$  we get from Eq. (4)  $a_{exp}^2 = 0.31 \cdot 10^{-3}$  for the maximal RHIC energy. Using numbers for the  $\sqrt{s_{NN}} = 200$  GeV reference case, from Eq. (5) we may quantify the  $\mathcal{CP}$  violation effect by the correlator

$$a^2 = K_{Au} (\sqrt{s_{NN}})^{-1/8} \cdot \tau_B . \quad (6)$$

The normalization constant  $K_{Au}$  can be tuned at the reference energy  $\sqrt{s_{NN}} = 200$  GeV from the inverse relation and experimental value  $a_{exp}$  at this energy for  $b = 10$  fm

$$K_{Au} = \frac{a_{exp}^2 \cdot (200)^{1/8}}{\tau_B(200)} . \quad (7)$$

The lifetime  $\tau_B$  may be defined as the time during which the magnetic field is above the critical value needed to support a fermion Landau level on the domain wall  $eB_{crit} = 2\pi/S_d$ , where  $S_d$  is the domain wall area. Since the size of the domain wall is not reliably known, it is hard to pin down the number, but it should be of the order of  $m_\pi^2$ . Honestly, we have to treat it as a free parameter.

Indeed the size of the topological defect (say, a sphaleron) in the region between  $T_c$  and  $2T_c$  is very uncertain. At weak coupling, the size is determined by the magnetic screening mass and it is  $\sim 1/(\alpha_s T)$ . If one plugs  $\alpha_s \approx 0.5$  and  $T = 200$  MeV, the size is of about 2 fm and then the threshold field is very small  $eB_y \sim (\alpha_s T)^2 \sim 0.2 m_\pi^2$ .

Table 1: Estimated parameters for the  $\mathcal{CP}$  violation effect in Au+Au collisions at centrality (40-50)% with the critical field  $eB_{crit} = 0.2 m_\pi^2$ .

$\sqrt{s_{NN}}$ GeV	$s_{NN}^{1/16}$	$\tilde{\tau}_B$ , fm/c	$\tau_\epsilon$ , fm/c	$a^2$
$4.5 \cdot 10^3$	2.86	0.018	$>1$	$0.016 \cdot 10^{-4}$
200	1.94	0.24	$>2$	$0.31 \cdot 10^{-3}$
130	1.84	0.33	$\sim 2.3$	$0.45 \cdot 10^{-3}$
62	1.68	0.62	$\sim 2.2$	$0.93 \cdot 10^{-3}$
17.9	1.43	1.41	$\sim 2.$	$2.48 \cdot 10^{-3}$
11.	1.35	1.66	$\sim 1.9$	$3.10 \cdot 10^{-3}$
4.7	1.21	0.	0.	0.

On the other hand, we know that between  $T_c$  and  $2T_c$  the magnetic screening mass which determines the size of the sphaleron is not small as expected from the perturbative theory,  $\alpha_s T$ , but from the lattice it is numerically large till about  $5T_c$ . This would increase the threshold to  $20 m_\pi^2$ , however the relation between magnetic mass and the sphaleron size is valid only as long as the coupling is weak. All we can say it is perhaps in between  $(0.2-20) m_\pi^2$ . Eventually lattice QCD calculations may clear this up.

The upper bound on the magnetic strength  $eB_{crit} = 20 m_\pi^2$  results in  $\tau_B = 0$  even for the RHIC energy and therefore in this case the CME should not be observable at all in this energy range. The time evolution of the magnetic field and energy density,  $\epsilon$ , of newly created hadrons are presented in Figs. 1 and 2. The extracted values of  $\tau_B$  defined by the constraints  $eB_y > 0.2 m_\pi^2$  and  $\tau_\epsilon$  ( $\epsilon > 1 \text{ GeV}/\text{fm}^3$ ) are summed in Tabl. 1. For the reference energy and the minimal magnetic field constraint we have  $K_{Au} = 2.52 \cdot 10^{-3}$ . If lifetimes are known for all energies one can estimate the  $\mathcal{CP}$  violation effect through the  $a^2$  excitation function.

From the first glimpse as follows from Tabl. 1, in the case of  $eB_{crit} = 0.2 m_\pi^2$  the interaction time  $\tau_B$  is defined solely by evolution of the magnetic field since  $\tilde{\tau}_B < \tau_\epsilon$  whereas  $\tau_\epsilon \approx 2 \text{ fm}$  independent of  $\sqrt{s_{NN}}$ . The expected CME for Au+Au at  $b = 10 \text{ fm}$  (see the last column in Tabl. 1) monotonously increases when  $\sqrt{s_{NN}}$  goes down but then sharply vanishes exhibiting a shallow maximum in the range between near the top SPS and NICA energies. The position of CME maximum and its magnitude depend on the cut level which just defines  $\tilde{\tau}_B$ . The decrease of the  $eB_y$  bound till  $0.02 m_\pi^2$  shifts the

maximum toward lower energy  $\sqrt{s_{NN}}$  and enhances its magnitude. In an opposite limit when results are extrapolated to the LHC energy, the CME falls down by a factor of about 20 with respect to the RHIC energy. This result is quite understandable. The CME is mainly defined by the relaxation time of the magnetic field which is concentrated in the Lorentz-contracted nuclear region  $\sim 2R/\gamma$ . Therefore, the CME is inversely proportional to the colliding energy,  $\sim 1/\sqrt{s_{NN}}$ , and proceeding from the RHIC to LHC energy we roughly get the suppression factor about  $4.5/0.2 \approx 22$ .

There is one worrying point here. Proceeding from  $\sqrt{s_{NN}} = 200$  to 62 GeV the predicted value of  $a^2$  for  $b=10$  fm increases in three times though not more 20% growth has been observed in these collisions in the recent experiment [6]. This essential disagreement cannot be removed by a simple variation of  $eB_{crit}$ . One may try to explain this correlator overestimation at  $\sqrt{s_{NN}} = 62$  GeV by an irrelevant choice of the energy dependence of multiplicity in Eq. (6). For the correlator ratio at these two energies we have

$$\frac{a^2(200)}{a^2(62)} = \frac{\tau_B(200)}{\tau_B(62)} \left( \frac{62}{200} \right)^{1/8} = 0.387 (0.31)^\beta \approx 0.72. \quad (8)$$

where we use lifetime values from Tabl. 1 and experimental values for correlators [6],  $\beta \equiv 1/8$ . As follows from Eq. (8), to explain the experiment the exponent should be negative,  $\beta < 0$ . Therefore, the fast growth of  $\tau_B$  with the energy decrease cannot be compensated by uncertainty in the energy dependence of the correlator  $a$ .

Uncertainty in the choice of the impact parameter does not help us to solve this issue. It turned out that one fails to fit this ratio by the variation of only  $eB_{crit}$ . Here we should remember that not only the strong magnetic field but also high density of soft equilibrium quark-gluon matter are needed. Equilibration requires some finite initial time  $t_{i,\varepsilon}$  which we associate with the moment when a maximum in the  $\varepsilon(t)$  is achieved (see Fig.2). This makes  $\tilde{\tau}$  shorter and in combination with  $eB_{crit}$  variation,  $\tau_B = \tilde{\tau}_B - t_{i,\varepsilon}$ , allows us to satisfy the condition (8). Using the value of  $\tau_B(200)$  obtained in this analysis one can recalculate the coefficient in Eq. (6),  $K_{Au} = 6.05 \cdot 10^{-3}$ , and therefore find the correlator  $a$  at any energy. In principle, similar analysis may be repeated for other impact parameters to consider the  $b$ -dependence of the CME. As was shown in Refs. [3] the CME roughly is linear in  $b/R$ . Taking this as a hypothesis we evaluate the centrality dependence of the CME fitting this line to points  $b = 10$  fm (or centrality (40 – 50)%) to be estimated in our model and  $b = 0$  where the CME is zero. The results are presented in Fig. 3 for Au+Au collisions at three energies.

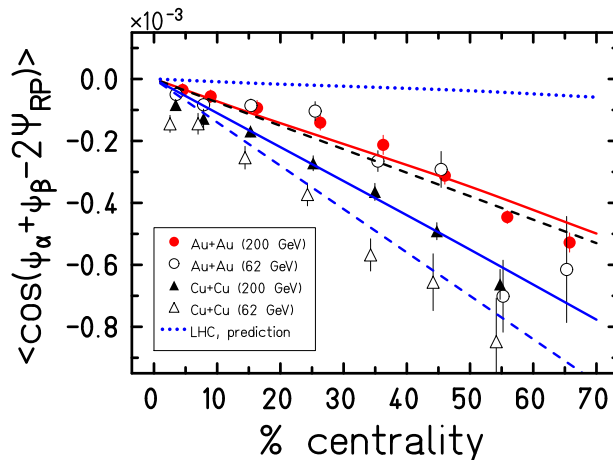


Figure 3: Centrality dependence of the CME. Experimental points for Au+Au and Cu+Cu collisions are from [6]. The dotted line is our prediction for Au+Au collisions at the LHC energy.

As it is seen the calculated lines quite reasonably reproduce the measured points of azimuthal asymmetry of charge separation for Au+Au collisions at  $\sqrt{s_{NN}} = 200$  and 62 GeV. The chosen value of  $eB_{crit} = 0.7 m_\pi^2$  results in absence of the CME at the top SPS energy because the critical magnetic field practically coincides with the maximal field at this bombarding energy (see Fig. 1). The CME at the LHC energy is expected to be less by a factor of about 20 as compared to that at the RHIC energy. Note that at the LHC energy we applied a simplified semi-analytical model [10] for magnetic field creation and assumed  $t_{i,\varepsilon} = 0$ . Thus, we consider this LHC estimate as an upper limit for the CME.

Similar analysis can be repeated for Cu+Cu collisions basing on available RHIC measurements at two collision energies. Here one remark is in order. An enhancement of the CME in Cu+Cu collisions with respect to Au+Au ones was seen experimentally at the same *centrality* [6] but not at the same *impact parameter*. As follows from the Glauber calculations, the impact parameter  $b=10$  fm for gold reactions corresponds to centrality (40-50)% while the same centrality for copper collisions matches  $b=4.2$  fm. The time distributions of the magnetic field and energy density for Cu+Cu collisions look very similar to that for Au+Au ones but lifetimes, both  $\tilde{\tau}_B$  and  $\tau_\varepsilon$ , are shorter in the Cu+Cu case. For the extracted lifetimes and other characteristics at  $eB_{crit} = 0.2 m_\pi^2$  ( $K_{Cu} = 6.34 \cdot 10^{-3}$ ) we meet again the same problem: one should compensate a too strong energy dependence of the model correla-

tors by the proper definition of lifetimes. Defining the lifetime in the same manner as for Au+Au collisions the lifetime ratio  $\tau_B(62)/\tau_B(200)$  is turned out to be very close to experimental one at  $eB_{crit} = 0.3 m_\pi^2$ . In this case  $K_{Cu} = 11.9 \cdot 10^{-3}$ . In the linear approximation with the reference point at  $b = 4.2$  fm, one may draw the centrality dependence of the CME for Cu+Cu collisions shown also in Fig.3 which is in a reasonable agreement with the experiment. Note that  $eB_{crit} = 0.3 m_\pi^2$  which is slightly above the maximal magnetic field at  $\sqrt{s_{NN}} = 62$  GeV implies that the CME for Cu+Cu collisions will not be observable even at the top SPS energy.

From dimensionality arguments the system-size dependence of the chiral magnetic effect (at the same all other conditions) would be expected to be defined by the surface  $S \equiv S_A(b)$  of an ‘‘almond’’-like transverse area of overlapping nuclei since both the high magnetic field and deconfined matter are needed for this effect. The magnetic field was evaluated in the the center of the overlapping region but as was shown in Ref. [10] the studied  $eB_y$  component is quite homogeneous along  $x$  of this ‘‘almond’’. Using for ‘‘almond’’ area a rough estimate as two overlapping discs of radius  $R = r_0 A^{1/3}$ , namely  $S \equiv S_A(b) = \pi \sqrt{R^2 - (b/2)^2} (R - b/2)$ , we have  $S_{Cu}(b = 4.2)/S_{Au}(b = 10) \approx 1.65$  which seems to be consistent with experimental ratio of the CME at  $\sqrt{s_{NN}}$  for these two points. However, this result was obtained for different  $eB_{crit}$  and non-zero initial time  $t_{i,\epsilon}$ , and this success cannot be repeated for Cu+Cu (62 GeV) collisions. Therefore, the Cu enhancement effect is not only a geometric one.

### 3 Towards a kinetic approach to the CME background

The discussed CME signal may originate not only from the spontaneous local CP violation but also be simulated by other possible effects. In this respect it is important to consider the CME background. We shall do that considering a full evolution of nucleus-nucleus collisions in terms of the HSD transport model [7] but including formation of electromagnetic field as well as its evolution and impact on particle propagation.

Generalized on-shell transport equations for strongly interacting particles in the presence of magnetic fields can be written as

$$\left\{ \frac{\partial}{\partial t} + (\nabla_{\vec{p}} \vec{U}) \nabla_{\vec{r}} - (\nabla_{\vec{r}} \vec{U} + q\vec{v} \times \vec{B}) \nabla_{\vec{p}} \right\} f(\vec{r}, \vec{p}, t) = I_{coll}(f, f_1, \dots, f_N)$$



which are supplemented by the wave equation for the magnetic field whose solution in the semi-classical approximation for point-like moving charges is reduced to the retarded Liénard-Wiechert potential used above [10]. The term  $U \sim \text{Re}(\Sigma^{ret})/2p_0$  is the hadronic mean-field.

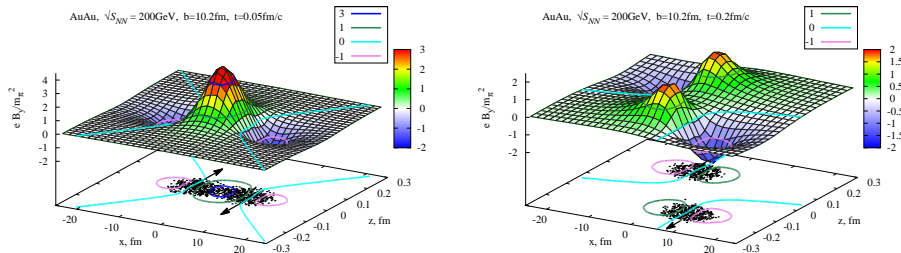


Figure 4: Distribution of the magnetic field strength  $eB_y$  in the  $y = 0$  plane at  $t = 0.05$  and  $0.2$  (in the middle)  $\text{fm}/c$  for Au+Au collisions at  $\sqrt{s_{NN}} = 200$  and  $b = 10.2$   $\text{fm}$ . The collision geometry is projected on  $x - z$  plane by points corresponding to a particular spectator position. Curves (and their projections) are levels of the constant  $eB_y$ .

One should note that the off-shell HSD transport approach is based not on the Boltzmann-like transport equation (9) but rather on the off-shell Kadanoff-Baym equations having similar general structure. The set of equations was solved in a quasiparticle approximation by using the Monte-Carlo parallel ensemble method. To find the magnetic field a space grid was used. In a lattice point of this grid the retarded vector potential is evaluated. The magnetic field is calculated by its numerical differentiation. The field inside a cell is approximated by that at the nearest grid point. To avoid singularities and self-interaction effects, particles within a given cell are excluded from procedure of the field calculation.

An evolution snapshot of the magnetic field  $B_y(x, y = 0, z, t)$  (in units of  $m_\pi^2$ ) formed in Au+Au (200 GeV) peripheral ( $b = 10.2$   $\text{fm}$ ) collisions are given in Fig.4 for two time moments  $t = 0.05$  and  $0.20$   $\text{fm}/c$ . The collisional geometry is presented by a set of points every of which corresponds to a spectator nucleon. The whole field is not homogeneous exhibiting a wide maximum over the transverse size of overlapping (participant) matter and strong contraction in longitudinal direction. Opposite rotation of the magnetic field along direction of two colliding nuclei results in corresponding two minima from outer sides of spectator matter remnants. At expansion these

remnants are moving away from each other. The position of a maximum in the magnetic field strongly correlates with that in the energy density of created particles. Large local values of  $B_y$  and  $\varepsilon$  reached in these Au+Au collisions provide necessary conditions for observation of signals of a possible parity violation.

## 4 Discussion and conclusions

Summarizing one should note that for heavy-ion collisions at  $\sqrt{s_{NN}} \gtrsim 11$  GeV the magnetic field and energy density of deconfined matter reach very high values which seem to be high enough for manifestation of the Chiral Magnetic Effect. However, these are only necessary conditions. To estimate a possible CME a particular model is needed. For the average correlator our qualitative prediction  $a^2 \sim s_{NN}^{-1/8}$  has a rather small exponent but nevertheless it is too strong to describe observable energy behavior of the CME. This model energy dependence can be reconcile with experiment [6] by a detailed treatment of the lifetime taking into account both the time of being in a strong magnetic field and time evolution of the energy density in the QGP phase. For the chosen parameters we are able to describe data for Au+Au collisions on electric charge separation at two available energies. We predict that the effect will be much smaller at the LHC energy and will sharply disappear near the top energy of SPS. Coming experiments at the Large Hadron Collider and that the planned Beam Energy Scan program at RHIC [12] are of great interest since they will allow one to test the CME scenario and to infer the critical magnetic field  $eB_{crit}$  governing by the spontaneous local  $\mathcal{CP}$  violation.

The experimentally observed CME enhancement for Cu+Cu collisions is related with the selection of different impact parameters for the same centrality. However, it is not reduced to a purely geometrical effect.

The problem of parity violation in strong interactions and the related CME are actively debated now. It is of great interest that the electric charge asymmetry with respect to the reaction plane may originate not only from the spontaneous local CP violation but also be simulated by other possible effects. First step in study of dynamical study of the CME background has been made in Sec.3. It is important that the developed kinetic approach in principle allows one to simulate the Chiral Magnetic effect itself. This work is in progress.

## Acknowledgements

Successful collaboration with D. Kharzeev, V. Skokov, E. Bratkovskaya, W. Cassing, V. Konchakovski and S. Voloshin is greatly acknowledged. We are thankful to V. Koch, R. Lacey, I. Selyuzhenkov, O. Teryaev and J. Thomas for comments. V.T. is partially supported by the DFG grant WA 431 8-1 RUSS and the Heisenberg-Landau grant. V.V. acknowledges financial support within the “HIC for FAIR” center of the “LOEWE” program.

## References

- [1] *Kharzeev D.* // Phys. Lett. B. 2006. V. 633. P.260.
- [2] *Kharzeev D. and Zhitnicky A.* // Nucl. Phys. A. 2007. V.797. P.67.
- [3] *Kharzeev D.E., McLerran L.D and Warringa H.J.* // Nucl. Phys. A. 2008. V.803. P.227.
- [4] *Fukushima K., Kharzeev D.E. and Warringa H.J* // Phys. Rev. D. 2008. V.78. P.074033.
- [5] *Kharzeev D.E. and Warringa Y.J.* // Phys. Rev. D. 2009. V.80. P.034028.
- [6] *Voloshin S. (STAR Collaboration)* // arXiv:0907.2213; *Abelev B.I., et al. (STAR Collaboration)* // arXiv:0909.1717; *Abelev B.I., et al. (STAR Collaboration)* // Phys. Rev. Lett. 2009. V.103. P.251601.
- [7] *Ehehalt W. and Cassing W.* // Nucl. Phys. A. 1996. V.602. P.449; *Bratkovskaya E.L and Cassing W.* // Nucl. Phys. A. 1997. V.619. P.413; *Cassing W. and Bratkovskaya E.L.* // Phys. Rept. 1999. V.308. P.65.
- [8] *Voloshin S.A.* // Phys. Rev. C. 2004. V.70. P.057901.
- [9] *Kharzeev D. and Nardi M.* // Phys. Lett. B. 2001. V.507. P.121.
- [10] *Skokov V., Illarionov A. and Toneev V.* // Int. J. Mod. Phys. A. 2009. V.24. P.5935.
- [11] *Bass S.A. et al.* // Prog. Part. Nucl. Phys. 1998. V.41. P.255.
- [12] *Odyniec G.* // J. Phys. G. 2010. V.27. P.094028.